

1 **Analysis of the thermal efficiency of a compound**
2 **parabolic Integrated Collector Storage solar**
3 **water heater in Kerman, Iran**

4
5 Rashid Panahi ¹, Mohammad Hassan Khanjanpour ², Akbar A. Javadi ²,
6 Mohammad Akrami ², Mohammad Rahnama ¹, Mehran Ameri ¹

7
8 ¹ Department of Mechanical Engineering, Shahid Bahonar University of Kerman,
9 Kerman, Iran

10 ² Department of Engineering, College of Engineering, Mathematics, and Physical
11 Sciences, University of Exeter, Exeter, United Kingdom

12
13
14 *Corresponding authors

15 *Akbar A. Javadi,

16 Harrison building, North Park Road, College of Engineering and Physical Sciences, University
17 of Exeter, EX4 4QF,

18 Phone: 01392723640,

19 A.A.Javadi@exeter.ac.uk

20
21 Keywords: Solar water heater; Integrated Collector Storage; Compound parabolic concentrators;
22 Thermal performance; Sustainable development

23 **Abstract**

24 This paper presents an experimental study involving the design, manufacturing and testing of a
25 prototype integrated collector storage (ICS) solar water heater (SWH) in combination with a
26 compound parabolic concentrator (CPC). The thermal efficiency of the developed system is
27 evaluated in Kerman (latitude 30.2907°N , longitude 57.0679°E), Iran. The developed system is
28 intended to supply hot water for a family in remote rural areas. A 6-month experimental study was
29 undertaken to investigate the performance of the ICS SWH system. The mean daily efficiency and
30 overnight thermal loss coefficient of each experiment were analyzed to examine the
31 appropriateness of these collectors for regions in Kerman. The results showed that mirror has the
32 highest mean daily efficiency (66.7%), followed by steel sheet (47.6%) and aluminum foil
33 (43.7%). The analysis of hourly and monthly operation diagrams for variations of water
34 temperature for the developed ICS system showed that by increasing the amount of radiation
35 entering the water heater, the thermal efficiency of the system decreases, such that the highest
36 efficiency was in April and the lowest in July. With the distribution of radiation intensity in the
37 months of August and September, the thermal efficiency of the system increased. This regional
38 study illustrates how selecting a proper concentrator can increase the thermal efficiency of this
39 solar-based system. It also shows how the temperature gradient between the ambient air and
40 internal water in the storage tank can influence the performance of such systems, and how a
41 controlled amount of hot water withdrawal can affect the system's efficiency. Developing the
42 ICSSWH system is an ideal sustainable solution in countries that benefit from a large amount of
43 solar intensity.

44

45

46

47 **Introduction**

48 Industrialization and population growth have caused a dramatic rise in the annual consumption of
49 fossil fuels [1]. Since 1859, most everyday energy usage relied directly or indirectly on fossil fuels.
50 This has caused many environmental problems such as global warming, acid rain, water pollution
51 and increased waste and environmental degradation. By implementing new technologies based on
52 utilizing renewable energy sources, the reliance on fossil fuels dwindles, and the contamination
53 caused by them can also be reduced. Planning and developing new energy sources to replace
54 fossil fuels has increased over the past two decades [2] to be used for different applications [3-6].
55 Solar energy is one of the more reliable sources of renewable energy and can provide 173,000 TW
56 of energy daily to the earth [7]. Although the amount of solar energy that reaches the ground is
57 abundant, its rate per unit area is low. A major challenge is therefore to collect and concentrate
58 this energy efficiently, which is usually done using solar water heaters.
59 Solar water heaters can be divided into two main categories: active and passive systems [8, 9].
60 The active system consists of a solar collector to absorb solar energy and a tank for storing hot
61 water. It includes three main types: direct, indirect, and drain back. In the direct systems, the water
62 circulates directly to the collector. When the temperature of the collector is greater than that of the
63 tank, a pump will circulate the water from the source to the collector. These systems are generally
64 not recommended for climate conditions that lead to cooling of the system or in cases that use
65 heavy or acidic water [10].
66 The indirect systems use antifreeze fluids such as propylene glycol in the collector for the purpose
67 of transferring the heat. The low freezing point of propylene glycol prevents the freezing of the
68 system and allows the solar systems to be used under conditions below 0 °C. The indirect systems
69 prevent the reverse flow of thermosiphon by using a one-way valve at night [11]. The third type

70 of active system is the water-back system. Water-back systems use water for heat transfer. To
71 prevent the risk of frost when the collector temperature is lower than the tank temperature, the
72 pump is switched off and the water inside the system returns to the reserve. The space inside the
73 collector is then filled with air, which protects against the freezing of the system [12].

74 Although active systems are relatively easy to set up, efficient passive systems are also utilized
75 based on their own capabilities. These are divided into two systems: Thermosiphon and ICS. The
76 Thermosiphon system uses high radiation absorption when it is heated (decreasing density). In this
77 system, a storage tank is installed at an altitude higher than the collector. When the water is heated,
78 it becomes lighter and naturally flows to the highest point inside the supply. The cold water from
79 the bottom of the source flows through the pipes to the bottom of the collector and creates a natural
80 circulation in the system. Circulation in the system stops when the temperature inside the collector
81 becomes lower than the temperature inside the tank. This prevents heat transfer from the system
82 to the environment at night when the temperature of the collector is lower than that of the supply
83 [13]. In the ICS type of passive SWHs, the storage tank and the collector are not separated from
84 each other. The cold water is directly connected to the collector and is heated by the sun. Unlike
85 other systems, hot water remains in the collector until it is consumed and then directly used by the
86 collector. ICS systems require larger storage sources (to increase radiation absorption capacity)
87 than conventional systems, which also protect the system against frost [14].

88 Many amendments have been made in recent years to various parts of the ICS system so that the
89 maximum absorption of radiation energy and the lowest thermal loss can be achieved
90 simultaneously for the system. From the early 1800s, a number of solar concentrators were built
91 to achieve higher temperatures and steam production [15]. The first ICS SWH was developed in
92 the southwest of the USA at the end of the 18th century. In 1982, Tiller and Wochatz analyzed the

93 performance of ICS water heaters in warm climates and discovered that ICS' performance is higher
94 than flat plate SWHs [16]. In another experimental study, a solar water heater (SWH) with a plastic
95 water bag (PWB) was designed and developed that produced desirable results in different weather
96 conditions [17]. In 1984, Faiman provided a standard method for calculating the efficiency of ICS
97 SWH water heaters [18]. This methodology helped Waller et al. [19] to analyze the rate of heat
98 loss in ICS solar water heaters. Rommel [20] concluded that transparent insulating materials can
99 increase the efficiency of ICS water heaters. Mohammed et al. [21] constructed an ICS SWH with
100 a buffer inside a repository, which showed better efficiency in comparison to non-buffer SWHs.
101 Tripanagnostopoulos & Souliotis [22] designed four different models with asymmetric geometries
102 by analyzing the system's heat loss during the night and their thermal performance. The results
103 were compared with the CPC concentrator. It was shown that the SWH with asymmetric geometry
104 had less thermal dissipation at night than the SWH with symmetrical geometry, and the system
105 with symmetric geometry had a higher efficiency than the others [22].

106 Regional studies were also planned to provide a database for governments and decision makers to
107 invest their budget wisely. One of these studies examined the resistance of a water heater to frost
108 in northern European climate conditions [23] to establish an economic evaluation of ICS water
109 heaters in mass production. In this study, the researchers analyzed the return on investment (ROI)
110 and showed that a large number of ICS water heaters was economical and also technically feasible
111 [24]. In 2003, Souliotis & Tripanagnostopoulos [25] conducted experiments on various ICS solar
112 water heaters. They constructed three water heaters with different CPM profiles with different
113 dams and showed that the SWH with a 30-cm droplet dryer had better thermal performance. In
114 another study, the temperature classification of ICS water heaters with a horizontal storage tanks
115 was experimentally evaluated to investigate the effects of multiple combinations of such systems

116 [26]. In 2008, Souliotis and Tripanagnostopoulos [27] analyzed the general distribution of water
117 in the tank wall of the heater. The results illustrated that the upper part of the source reserve
118 absorbed the majority of the reflected radiation. The first study on optical performance of an ICS
119 heater was published in 2015 [28]. The results of this study provided a significant improvement in
120 optical efficiency and the distribution of radiation absorption with various solar slope angles. In
121 the following year, the same researchers optimized the geometrical characteristics of an ICS SWH
122 system in order to find the optimal thermal performances [29]. Most recently, Harmim et al. [30]
123 simulated and tested an ICS SWH for integration into a building façade. Their system had a daily
124 efficiency between 36.4 and 51.6% and its thermal loss coefficient during night-time was between
125 2.17 and 3.12W. The results from these studies showed that different regions receive different
126 amounts of energy based on their assigned latitudes.

127 Because of their location, some countries have benefited from a greater amount of solar intensity
128 [31]. One of these countries is Iran, which is located at a latitude of between 25 to 40 degrees
129 North. The amount of solar radiation in Iran is estimated to be between 1800 and 2200 kWh/m²
130 per year, which is higher than the global average [32]. In Iran, on average more than 280 days per
131 year are sunny, which is higher than a vast majority of the countries within Europe [33]. Therefore,
132 it can rely on different forms of solar energy solution to generate electricity and provide the heating
133 requirements for residential homes. By analyzing all sites of Iran, Shiraz, Yazd and Kerman have
134 areas with higher solar radiation, as illustrated in the solar GIS map [34]. Unfortunately, due to the
135 fact that Iran has one of the largest endowment of oil and natural gas resources in the world [35],
136 most of the population of these regions are already utilizing natural gas for heating water [36]. In
137 this regional study, the Kerman Province, which has 23 cities and encompasses more than 11% of
138 Iran's terrestrial area, was selected for investigation [37]. In addition, its vicinity to the Lut Desert,

139 lower population density and abundance of remote villages compared to its neighboring provinces
140 are other features making it apt for investigating solar water heaters [38]. Although the
141 technologies to generate electricity such as photovoltaic (PV) panels started being used in Iran, the
142 applications of solar water heaters has hitherto received little to no attention. This technology can
143 be widely used to provide heating water for consumer or industrial demands in Kerman province,
144 having a great value of solar radiance comparing against the rest of them (See Fig. 1) [39].

145
146 The system presented in this paper has several advantages: it is economically affordable,
147 structurally robust and easy to manufacture and install using local material, especially in
148 developing countries.

149 Although there have been some studies on ICS SWH system in some parts of the world, the
150 findings cannot be easily extended to other specific regions. Furthermore, long-term experiments
151 on the performance and efficiency of ICS SWH systems is rare in the literature. Therefore, this
152 paper

153
154
155 In the following sections, the design and testing processes for an ICS SWH system for Kerman
156 Province is presented and discussed.

157

158 **2. Geometric design of the ICS SWH system**

159 **2.1. Storage tank**

160 The storage tank is the central part of the ICS SWH system. Its function is to absorb solar radiation
161 and transfer the thermal energy to the stored water. The size and shape of a storage tank have an

162 important effect on the absorption of solar energy. The greater the area of the storage tank exposed
163 to the sun, the less time it takes to warm the water. However, in a normal climate, a high-surface
164 storage tank will lose a significant part of the energy through heat transfer and radiation with long
165 wavelengths, and mostly during the night due to heat loss to the surroundings [40]. According to
166 the study carried out by Keshavarzia et al. [41], water consumption in rural regions of Iran is about
167 120 l/d per person. In order to supply this amount of household water, the diameter and length of
168 the storage tank were chosen as 30 cm and 200 cm respectively, resulting in a storage tank volume
169 of just over 141 l. The storage tank should be made of high conductivity material such as
170 aluminum, copper or galvanized iron/steel [42]. The thickness of the sheet should be chosen such
171 that it withstands the pressure of the water, in addition to having low thermal resistance against
172 heat transfer [40]. Considering the available sheets in the market, a thickness of 1 mm was chosen.

173

174

175 **2.2. Geometry of CPC concentrator**

176 A symmetric CPC concentrator was selected to achieve the highest efficiency based on literature
177 [22] (see Fig. 2).

178

179 Fig. 2 - Cross-section view of a symmetric CPC [22]

180

181 In such models, the concentrator is composed of four parts: AB, BC, C'D, and DA' (see Fig. 2).

182 The parabolic equations for the different parts are as follows [22]:

183 Part 1 (AB):

184 $X = -r_T[1 + \pi \sin \psi / (1 + \cos \psi)]$ (1)

185 $Y = -r_T[\pi \cos \psi / (1 + \cos \psi)]$ (2)

186 Part 2 (BC)

187 $X = -r_T(\sin \omega - \cos \omega)$ (3)

188 $Y = -r_T(\cos \omega + \sin \omega)$ (4)

189 Part 3: (C'D):

190 $X = r_T(\cos \acute{\omega} + \acute{\omega} \sin \acute{\omega})$ (5)

191 $Y = r_T(\sin \acute{\omega} - \acute{\omega} \cos \acute{\omega})$ (6)

192 Part 4 (DA '):

193 $X = r_T \pi \cos \acute{\psi} / (1 + \cos \acute{\psi})$ (7)

194 $Y = r_T[1 + \pi \sin \acute{\psi} / (1 + \cos \acute{\psi})]$ (8)

195

196 where: ω : involute concentrator's angle; $\acute{\omega}$: upper involute concentrator's angle; ψ : parabolic
 197 concentrator's angle; $\acute{\psi}$: upper parabolic concentrator's angle; $\acute{\psi} = \psi = 58$ degrees and $\omega =$
 198 $\acute{\omega} = 90$ degrees [22].

199 The width of the concentrator ($W\alpha$) is $AA' = BD = 2\pi r_T$ [22]. As the radius of the storage tank
 200 (r_T) was chosen as 15 cm, $W\alpha$ is 95 cm and the length of the aperture (L_α), which is equal to the
 201 length of the storage tank (L_T), is 200 cm. This results in the aperture area (A_α) of 16,500 cm² for
 202 the SWH system. To obtain the exact dimensions of the curves, a computer program was written

203 based on the above equations to calculate the coordinates of the points for each degree of variation
204 of ψ and ω . The system specification is presented in Table 1.

205

206 Table 1: Configuration details of the tested ICS SWH

207

208 where: D_T : Diameter of the storage tank; V_T : Volume of the storage tank, A_r : area of absorber;
209 CR: concentration ratio.

210 It should be noted that the concentrator should not oxidize during operation as it will reduce its
211 smoothness. In the market, polished sheets that have high reflection properties include mirrors
212 [13], steel sheets and aluminum foil. Each of the three concentrators was installed on the water
213 heater, and various experiments were carried out to ultimately select the concentrator that had the
214 best thermal performance. The general characteristics of the designed ICS SWH are summarized
215 in Table 2.

216

217 Table 2: General characteristics of the water heater

218

219 3. Construction and assembly

220 Based on the results obtained in the previous section, an ICS SWH with a symmetric CPC
221 concentrator was developed (Figs. 3 and 4). The structure of an ICS SWH should be light and
222 portable, and also compatible with local climatic conditions. Therefore, chipboard was selected to
223 build the structure of the SWH. As the system should be thermally insulated, the structure was
224 covered with glass wool. To ensure the water heater's screen was always perpendicular to the
225 incoming sunlight, a manual sun tracker system was placed in the back of the water heater, which

226 was able to adjust the position of the regulator to desired angles (Fig. 4). This allowed to the angle
227 of the water heater to be changed daily, monthly or seasonally, for maximum efficiency. It should
228 be noted that this angle would change with the latitude of the area where it is installed.

229

230 Fig. 3 – Construction and assembly of the ICS SWH system

231

232 4. Experimental analysis and data collection

233 4.1. Thermal performance of concentrators

234 The mean daily efficiency of the system can be determined as [43].

$$235 \quad \eta_d = Q_W / Q_R \quad (9)$$

236 where: η_d : mean daily efficiency; Q_W : heat in water storage tank; Q_R : integrated solar radiation
237 on the system aperture. The value of Q_W without any water drainage during the day is determined
238 as:

$$239 \quad Q_W = M_w C_{p,w} (T_1 - T_0) \quad (10)$$

240 where: M_w : mass of water; $C_{p,w}$: specific heat of water; T_0 : initial storage water temperature; T_1 :
241 final storage water temperature.

242 The total amount of solar radiation entering the aperture area of SWH during the day (from time
243 t_0 (7:00) to time t_1 (19:00)), is obtained by integrating the intensity field $G(t)$ [44]:

$$244 \quad Q_R = A_a \int_{t_0}^{t_1} G(t) dt \quad (11)$$

$$245 \quad G_m = (\int_{t_0}^{t_1} G(t) dt) / Dt \quad (12)$$

246 where: G_m : mean daily solar radiation intensity; Dt: time interval during daily operation.

247 Therefore, the mean daily efficiency can be determined as a function of the
248 ratio DT_{mD}/G_m ($Kw^{-1}m^2$), by second-degree polynomial fitting [45]:

$$249 \quad \eta_d = C + B(DT_{mD}/G_m) + A (DT_{mD}/G_m)^2 \quad (13)$$

250 where: $DT_{mD} = ((T_0 + T_1)/2) - T_{ma}$; T_{ma} : mean ambient temperature. The coefficient C represents
251 the mean daily efficiency of the system in the case of $(T_0 + T_1)/2 = T_{ma}$, and A, B are the thermal
252 loss parameters of the system during the daily operation [46].

253 For night time operation, the thermal losses of the system are considered to be introduced with the
254 parameter U_s , which expresses the thermal performance of the system from afternoon until the
255 following morning, when the system does not catch any solar radiation. The night-time heat loss
256 coefficient (U_s) can be calculated by the following equation [47]:

$$257 \quad U_s = (\rho C_{p,w} V_T / Dt) \ln[(T_{0m} - T_{am}) / (T_{1m} - T_{am})] \quad (14)$$

258 where: V_T : the volume of storage tank; ρ : density of water; Dt: time interval; T_0 : mean initial
259 storage water temperature; T_1 : mean final storage water temperature; T_{am} : mean ambient
260 temperature.

261 Fig. 4: The constructed ICS SWH at the testing site in Kerman

262

263 4.2. Measurement apparatus

264 A k-type thermocouple was used to measure the temperature of the water, T_w and the ambient
265 temperature, T_a , with the accuracy of ± 1.5 °C for temperature range of 0-200 °C. A Kipp and
266 Zonen pyranometer (Model: CMP22) was utilised to measure the radiation input to the collector.

267 The accuracy of the exploited pyranometer was $\pm 5 \text{ W/m}^2$. All the gathered data was collected
268 using a data logger (Model: ST-8891E) and compiled using the linked laptop to the data logger.

269

270 **4.3. Data collection and error analysis**

271 Following collecting water temperature and solar radiation intensity, the raw data was converted
272 into meaningful information depicting by the relevant graphs to analyze the rate of change and
273 observe the performance in hourly manner. The source of error was mainly based on the equipment
274 during the experiments. The variations of overnight thermal loss coefficients and mean daily
275 efficiency were fitted with linear and second-order polynomial trendlines, respectively.
276 Accordingly, the amount of errors of each curve-fitting by model of R-squared (coefficient of
277 determination) were calculated and they were placed in relevant tables (Tables 3, 4, 6 and 7).

278

279 **4.4. Selection and testing of the concentrator**

280 To achieve optimal performance, selecting a proper concentrator has an important effect on the
281 thermal efficiency of the solar system [48]. Experiments were carried out with the installation of
282 different concentrators on the system and the evaluation of their thermal performances. Based on
283 the available material for concentrators in the market, mirror, steel sheet, and aluminum foil were
284 selected. The first experiment was performed by installing the aluminum foil on the system and
285 testing for three consecutive days (see Fig. 5). The water temperature at the start (of all tests) was
286 $21 \text{ }^\circ\text{C}$. On the first day of the test, the temperature of the water inside the storage tank reached 43
287 $^\circ\text{C}$ while on the second and third days it reached $53 \text{ }^\circ\text{C}$ and $61 \text{ }^\circ\text{C}$ respectively. By replacing the

288 concentrator and installing the steel sheet or mirror, the temperature of the water inside the storage
289 tank increased throughout the day (see Fig. 5).

290

291 Fig. 5 - Temperature changes for three consecutive days (M_b : Mirror booster , A_f : Aluminum
292 foil, S_s : Steel sheet, T_a : ambient temperature , G : incoming solar radiation intensity)

293

294 Fig. 6 – Overnight thermal loss coefficients and mean daily efficiency (M_b : \square , A_f : \circ , S_s : \blacktriangle)

295

296 It can be seen from Fig. 5 that the temperature reduction during the night was the highest for the
297 mirror. The variations of overnight thermal loss coefficients and mean daily efficiency are plotted
298 in Fig. 6. By fitting a second-order polynomial function [49] to the points obtained, an equation
299 for the mean daily efficiency was obtained for each material (Table 3). According to the equations
300 in Table 3, the coefficient C of mean daily efficiency equations was highest (0.667) for the mirror,
301 and it was 0.476 for the steel sheet and 0.437 for the aluminum foil. This indicates that the output
302 of the mirror was better than the steel sheet and aluminum foil during the day.

303

304 Table 3. Equations of mean daily efficiency of concentrators

305

306 In the same way, a first-order line [49] was fitted for the obtained points of the thermal loss
307 coefficient, and the equations for the 3 concentrators are shown in Table 4. The main part of
308 equation [43] is 6.9877 for the aluminum foil, 8.0035 for the steel sheet and 11.016 for the mirror.

309 The results indicate that, although the steel sheet has the second highest efficiency among the
310 experimented materials, it has an acceptable heat loss in compression with the mirror. In addition,
311 it is cheaper and easy to install [24]. Therefore, the steel sheet was selected in the ICS SWH system
312 for monthly experiments (see Fig. 6).

313

314 Table 4. Equations of overnight thermal loss coefficient (U_s) for different concentrators

315

316

317 **4.5. Thermal performance of the ICS SWH in 6 different months in Kerman**

318 Since the solar slope angle changes every month, the angle of the ICS SWH needs to be adjusted
319 to obtain maximum solar radiation. Table 5 provides the optimal angles for obtaining the highest
320 solar radiation for some Iranian cities [50]. According to this table, for Kerman, the optimal angle.

321

322 Table 5 - The solar slope angles in degree ($^{\circ}$) at different months for 6 cities in Iran [50]

323

324 changes by about 7 to 8 degrees in every month. For each month, the data of the temperature
325 changes (the ambient temperature and temperature of the water in the storage tank) and the amount
326 of radiation entering the system for three consecutive days were collected and the results are
327 plotted in Fig. 7. Then, using equations (13) and (14), the mean daily efficiency and overnight
328 thermal loss coefficients were determined at different time intervals and the results are plotted in
329 Fig. 8. The equations of mean daily efficiency and overnight thermal loss coefficient by fitting the
330 obtained points are evaluated for 6 different months (see Tables 6 & 7).

331

332 Table 6: The system's mean daily efficiency (η_d) in different months in Kerman

333

Table 7: Overnight heat loss coefficient of the system (U_s) in different months in Kerman

334

335 The first monthly test was carried out in April and according to Table 4, the ICS SWH was adjusted
336 with solar slope angle ($\beta=14.55^\circ$). The water temperature was 21 °C at the start of the test and the
337 temperature of the water reached 65 °C on the third day of the experiment. The recorded
338 temperature changes in April are presented in Fig. 7.

339

340 Fig. 7 – T_w ■■■, T_a ■■■ and G ■■■ for three consecutive days in 6 different months

341

342 By using the efficiency equation, the coefficients C, B, and A were determined and shown in Fig.
343 8. The coefficient C is defined as the maximum efficiency of the ICS SWH system, which
344 according to the results obtained, is 0.6557. Similarly, considering Equation 14, the heat loss
345 coefficient of ICS SWH was obtained during the night (see Fig. 8).

346

347 Fig. 8 – Mean daily efficiency (left) and heat loss coefficient (right) of ICS SHW in Kerman (6
348 mounts)

349

350 In May, with the warming of the climate and changing angle of the sun, according to Table 4 for
351 Kerman (β was set to 77.1°), the ICS SHW system was tested. The pyranometer recorded a solar
352 radiation intensity of 980 W/m^2 in May. The water temperature in the storage tank reached 72°C .
353 Fig. 7 shows the temperature changes for three consecutive days. The mean daily efficiency and
354 heat loss coefficient graphs are presented in Fig. 8, and the relevant equations are listed in Tables
355 6 and 7. The coefficient C for May is 0.6129, which is less than the value in April.

356 The third test was conducted in June at a slope angle of -4.89° (slope to the North). The
357 temperature changes on three consecutive days are shown in Fig. 7. The maximum temperature of
358 the water was measured as 73°C , which was more than for the three days of the experiments in
359 April and May.

360 For testing in July, the water heater angle was set to -2.8° . The maximum solar radiation intensity
361 that the pyranometer displayed was 1120 W/m^2 . The temperature of the water after three days of
362 testing reached 74°C , and the difference between the water temperature at the start and end of the
363 test was 52°C , which was the highest difference compared to the earlier recorded months. Looking
364 at the coefficient C in the equations (Table 7), the test carried out in July has the smallest amount
365 of heat loss. To evaluate the thermal performance of the system in August, the acceptance angle
366 of the system (α) was adjusted to 83.93° . The sun's radiation intensity declined in comparison with
367 July, and hence, this month can be considered as a turning point in terms of solar radiation. Mean
368 daily performance also rose in August, whereas it had gone down in the previous months, which
369 can also be considered as a turning point in the ICS SWH. The last test was carried out in
370 September at an angle of $\beta=26.63^\circ$. The highest temperature changes for the first, second and third
371 days of the experiment were 31°C , 13.5°C , and 21°C respectively. In September, the coefficient
372 C and the efficiency of the water heater increased (See Fig. 9).

373

374 Fig. 9 – Thermal efficiency of the ICS SWH and mean daily radiation in 6 different months in
375 Kerman, Iran

376

377 **5. Conclusion**

378 This paper presented the design, fabrication and testing of an ICS SWH system for Kerman in Iran.
379 The developed ICS SWH can be used to heat water in houses or preheat water in small to medium-
380 sized industries. The main advantages of this system, compared with the available models on the
381 market, are inexpensive materials and portability. The developed system provides an alternative
382 solution for heating water, especially in remote rural areas.

383 The tested ICS SWH showed acceptable efficiency in comparison with similar systems [40].
384 Looking at the changes in coefficient C (Table 6), it can be noted that by increasing the amount of
385 radiation entering the water heater, the thermal efficiency of the system decreases, such that the
386 highest efficiency was in April and the lowest was in July. With the distribution of radiation
387 intensity in the months of August and September, the thermal efficiency of the system increased.
388 Based on these results, the highest efficiency would be in the colder months or in colder regions.
389 This is in agreement with the results reported in [51].

390 By increasing solar radiation intensity, the capacity of energy absorption of the system decreased,
391 since a temperature gradient rise will increase the heat loss due to convective heat transfer and
392 radiation [52]. Also, the results shows that by increasing the temperature of the water in the storage
393 tank, the radiated heat loss from the system increases.

394 One of the influential parameters on the system's performance is the temperature gradient between
395 the ambient air and water inside the storage tank. The results of this study showed that by
396 increasing the ambient temperature in hot climatic conditions such as those of Kerman, the radiated
397 energy potential in the system decreases. Therefore, constant withdrawal of hot water from the
398 tank can be recommended to help increase efficiency.

399 The results of the experiments with the three common concentrators – mirror booster, steel sheet
400 and aluminum foil – showed that using mirror reflection can increase the thermal efficiency of the
401 system, but on the other hand, can lead to more thermal losses in the system. The steel sheet is the
402 optimal amongst the materials tested, as it is economically affordable, stronger and also easy to
403 install in rural areas in Kerman.

404 **Funding**

405 None.

406 **Declaration of Competing Interest**

407 None declared.

408 **Acknowledgement**

409 The authors would like to appreciate the anonymous reviewers for their insightful comments and
410 suggestions.

411

412 **References**

- 413 1. Quaschnig, V.V., *Renewable Energy and Climate Change, 2nd Edition*. 2019: Wiley.
- 414 2. Khare, V., S. Nema, and P. Baredar, *Solar–wind hybrid renewable energy system: A*
415 *review*. *Renewable and Sustainable Energy Reviews*, 2016. 58: p. 23-33.

- 416 3. Alotaibi, D.M., M. Akrami, M. Dibaj, and A.A. Javadi, *Smart energy solution for an*
417 *optimised sustainable hospital in the green city of NEOM*. Sustainable Energy
418 Technologies and Assessments, 2019. 35: p. 32-40.
- 419 4. de Freitas Viscondi, G. and S.N. Alves-Souza, *A Systematic Literature Review on big data*
420 *for solar photovoltaic electricity generation forecasting*. Sustainable Energy Technologies
421 and Assessments, 2019. 31: p. 54-63.
- 422 5. Sow, A., M. Mehrtash, D.R. Rouse, and D. Haillot, *Economic analysis of residential solar*
423 *photovoltaic electricity production in Canada*. Sustainable Energy Technologies and
424 Assessments, 2019. 33: p. 83-94.
- 425 6. Chilundo, R.J., D. Neves, and U.S. Mahanjane, *Photovoltaic water pumping systems for*
426 *horticultural crops irrigation: Advancements and opportunities towards a green energy*
427 *strategy for Mozambique*. Sustainable Energy Technologies and Assessments, 2019. 33: p.
428 61-68.
- 429 7. Garcia, A.G., N. Sras, and M. Zuhir, *Energy Resources Analysis*. 2017.
- 430 8. Patel, K., P. Patel, and J. Patel, *Review of solar water heating systems*. International Journal
431 of Advanced Engineering Technology, 2012. 3(4): p. 146-149.
- 432 9. Hohne, P., K. Kusakana, and B. Numbi, *A review of water heating technologies: An*
433 *application to the South African context*. Energy Reports, 2019. 5: p. 1-19.
- 434 10. Shukla, R., K. Sumathy, P. Erickson, and J. Gong, *Recent advances in the solar water*
435 *heating systems: A review*. Renewable and Sustainable Energy Reviews, 2013. 19: p. 173-
436 190.
- 437 11. Chan, H.-Y., S.B. Riffat, and J. Zhu, *Review of passive solar heating and cooling*
438 *technologies*. Renewable and Sustainable Energy Reviews, 2010. 14(2): p. 781-789.
- 439 12. Gautam, A., S. Chamoli, A. Kumar, and S. Singh, *A review on technical improvements,*
440 *economic feasibility and world scenario of solar water heating system*. Renewable and
441 Sustainable Energy Reviews, 2017. 68: p. 541-562.
- 442 13. Jamali, H., *Investigation and review of mirrors reflectance in parabolic trough solar*
443 *collectors (PTSCs)*. Energy Reports, 2019. 5: p. 145-158.
- 444 14. Jamar, A., Z. Majid, W. Azmi, M. Norhafana, and A. Razak, *A review of water heating*
445 *system for solar energy applications*. International Communications in Heat and Mass
446 Transfer, 2016. 76: p. 178-187.

- 447 15. Fernández-García, A., E. Zarza, L. Valenzuela, and M. Pérez, *Parabolic-trough solar*
448 *collectors and their applications*. Renewable and Sustainable Energy Reviews, 2010.
449 14(7): p. 1695-1721.
- 450 16. Tiller, J. and V. Wochatz. *Performance of integrated passive solar water heaters*
451 *(Breadbox-type) under varying design conditions in the South-eastern US*. in *Proceedings*
452 *of the Seventh National Passive Solar Conference, Knoxville, TN, USA*. 1982.
- 453 17. Garg, H., G. Datta, and A. Bhargava, *Studies on an all plastic solar hot water bag*.
454 *International journal of energy research*, 1984. 8(3): p. 291-296.
- 455 18. Faiman, D., *Towards a standard method for determining the efficiency of integrated*
456 *collector-storage solar water heaters*. Solar energy, 1984. 33(5): p. 459-463.
- 457 19. Weller, P., G. Clark, and W. Collins. *Indoor testing of an integral passive solar water*
458 *heater*. in *Proceedings of the 10th national passive solar conference*. 1985.
- 459 20. Rommel, M. and A. Wagner, *Application of transparent insulation materials in improved*
460 *flat-plate collectors and integrated collector storages*. Solar energy, 1992. 49(5): p. 371-
461 380.
- 462 21. Mohamad, A., *Integrated solar collector–storage tank system with thermal diode*. Solar
463 *Energy*, 1997. 61(3): p. 211-218.
- 464 22. Tripanagnostopoulos, Y. and M. Souliotis, *Integrated collector storage solar systems with*
465 *asymmetric CPC reflectors*. Renewable Energy, 2004. 29(2): p. 223-248.
- 466 23. M. Smyth , P.C.E., B. Norton, *Evaluation of a freeze resistant integrated collector/storage*
467 *solar water-heater for northern Europe*. Applied Energy, 2001. 68: p. 265-274.
- 468 24. Smyth, M., P. Eames, and B. Norton, *Techno-economic appraisal of an integrated*
469 *collector/storage solar water heater*. Renewable Energy, 2004. 29(9): p. 1503-1514.
- 470 25. Souliotis, M. and Y. Tripanagnostopoulos, *Experimental study of CPC type ICS solar*
471 *systems*. Solar Energy, 2004. 76(4): p. 389-408.
- 472 26. Assari, M.R., H.B. Tabrizi, and M. Savadkohy, *Numerical and experimental study of inlet-*
473 *outlet locations effect in horizontal storage tank of solar water heater*. Sustainable Energy
474 *Technologies and Assessments*, 2018. 25: p. 181-190.
- 475 27. Souliotis, M. and Y. Tripanagnostopoulos, *Study of the distribution of the absorbed solar*
476 *radiation on the performance of a CPC-type ICS water heater*. Renewable Energy, 2008.
477 33(5): p. 846-858.

- 478 28. Benrejeb, R., O. Helal, and B. Chaouachi, *Optical and thermal performances improvement*
479 *of an ICS solar water heater system*. Solar Energy, 2015. 112: p. 108-119.
- 480 29. Benrejeb, R., O. Helal, and B. Chaouachi, *Optimization of the geometrical characteristics*
481 *of an ICS solar water heater system using the two-level experience planning*. Applied
482 Thermal Engineering, 2016. 103: p. 1427-1440.
- 483 30. Harmim, A., M. Boukar, M. Amar, and A. Haida, *Simulation and experimentation of an*
484 *integrated collector storage solar water heater designed for integration into building*
485 *facade*. Energy, 2019. 166: p. 59-71.
- 486 31. Clifford, M. and D. Eastwood, *Design of a novel passive solar tracker*. Solar Energy, 2004.
487 77(3): p. 269-280.
- 488 32. Nejad, R.M., *A survey on performance of photovoltaic systems in Iran*. Iranica Journal of
489 Energy & Environment, 2015. 6(2): p. 77-85.
- 490 33. Rahimzadeh, F., M. Pedram, and M.C. Kruk, *An examination of the trends in sunshine*
491 *hours over Iran*. Meteorological Applications, 2014. 21(2): p. 309-315.
- 492 34. Enjavi-Arsanjani, M., K. Hirbodi, and M. Yaghoubi, *Solar energy potential and*
493 *performance assessment of CSP plants in different areas of Iran*. Energy Procedia, 2015.
494 69: p. 2039-2048.
- 495 35. Ghorashi, A.H. and A. Rahimi, *Renewable and non-renewable energy status in Iran: Art*
496 *of know-how and technology-gaps*. Renewable and Sustainable Energy Reviews, 2011.
497 15(1): p. 729-736.
- 498 36. Heidari, H., S.T. Katircioglu, and L. Saeidpour, *Natural gas consumption and economic*
499 *growth: Are we ready to natural gas price liberalization in Iran?* Energy Policy, 2013. 63:
500 p. 638-645.
- 501 37. Hamid, B., A. Mohammad Bagher, B. Mohammad Reza, and B. Mahboubeh, *Review of*
502 *sustainable energy sources in Kerman*. World Journal of Engineering, 2016. 13(2): p. 109-
503 119.
- 504 38. Roya, N. and B. Abbas, *Colorectal cancer trends in Kerman province, the largest province*
505 *in Iran, with forecasting until 2016*. Asian Pacific Journal of Cancer Prevention, 2013.
506 14(2): p. 791-793.

- 507 39. Besarati, S.M., R.V. Padilla, D.Y. Goswami, and E. Stefanakos, *The potential of*
508 *harnessing solar radiation in Iran: Generating solar maps and viability study of PV power*
509 *plants*. Renewable energy, 2013. 53: p. 193-199.
- 510 40. Smyth, M., P. Eames, and B. Norton, *Integrated collector storage solar water heaters*.
511 Renewable and Sustainable Energy Reviews, 2006. 10(6): p. 503-538.
- 512 41. Keshavarzi, A., M. Sharifzadeh, A.K. Haghghi, S. Amin, S. Keshtkar, and A. Bamdad,
513 *Rural domestic water consumption behavior: A case study in Ramjerd area, Fars province,*
514 *IR Iran*. Water research, 2006. 40(6): p. 1173-1178.
- 515 42. Kenisarin, M. and K. Mahkamov, *Solar energy storage using phase change materials*.
516 Renewable and sustainable energy reviews, 2007. 11(9): p. 1913-1965.
- 517 43. Souliotis, M., S. Kalogirou, and Y. Tripanagnostopoulos, *Modelling of an ICS solar water*
518 *heater using artificial neural networks and TRNSYS*. Renewable Energy, 2009. 34(5): p.
519 1333-1339.
- 520 44. Helal, O., B. Chaouachi, and S. Gabsi, *Design and thermal performance of an ICS solar*
521 *water heater based on three parabolic sections*. Solar Energy, 2011. 85(10): p. 2421-2432.
- 522 45. Tripanagnostopoulos, Y. and M. Souliotis, *ICS solar systems with two water tanks*.
523 Renewable Energy, 2006. 31(11): p. 1698-1717.
- 524 46. Tripanagnostopoulos, Y. and M. Souliotis, *ICS solar systems with horizontal (E-W) and*
525 *vertical (N-S) cylindrical water storage tank*. Renewable Energy, 2004. 29(1): p. 73-96.
- 526 47. Tripanagnostopoulos, Y. and M. Souliotis, *ICS solar systems with horizontal cylindrical*
527 *storage tank and reflector of CPC or involute geometry*. Renewable Energy, 2004. 29(1):
528 p. 13-38.
- 529 48. Harris, J.A. and T.G. Lenz, *Thermal performance of solar concentrator/cavity receiver*
530 *systems*. Solar energy, 1985. 34(2): p. 135-142.
- 531 49. Garnier, C., T. Muneer, and J. Currie, *Numerical and empirical evaluation of a novel*
532 *building integrated collector storage solar water heater*. Renewable energy, 2018. 126: p.
533 281-295.
- 534 50. Talebizadeh, P., M. Mehrabian, and M. Abdolzadeh, *Determination of optimum slope*
535 *angles of solar collectors based on new correlations*. Energy Sources, Part A: Recovery,
536 Utilization, and Environmental Effects, 2011. 33(17): p. 1567-1580.

- 537 51. Dieng, A. and R. Wang, *Literature review on solar adsorption technologies for ice-making*
538 *and air-conditioning purposes and recent developments in solar technology*. Renewable
539 and sustainable energy reviews, 2001. 5(4): p. 313-342.
- 540 52. Kumar, R. and M.A. Rosen, *Thermal performance of integrated collector storage solar*
541 *water heater with corrugated absorber surface*. Applied Thermal Engineering, 2010.
542 30(13): p. 1764-1768.

543

544

545

546

547

548

549

550

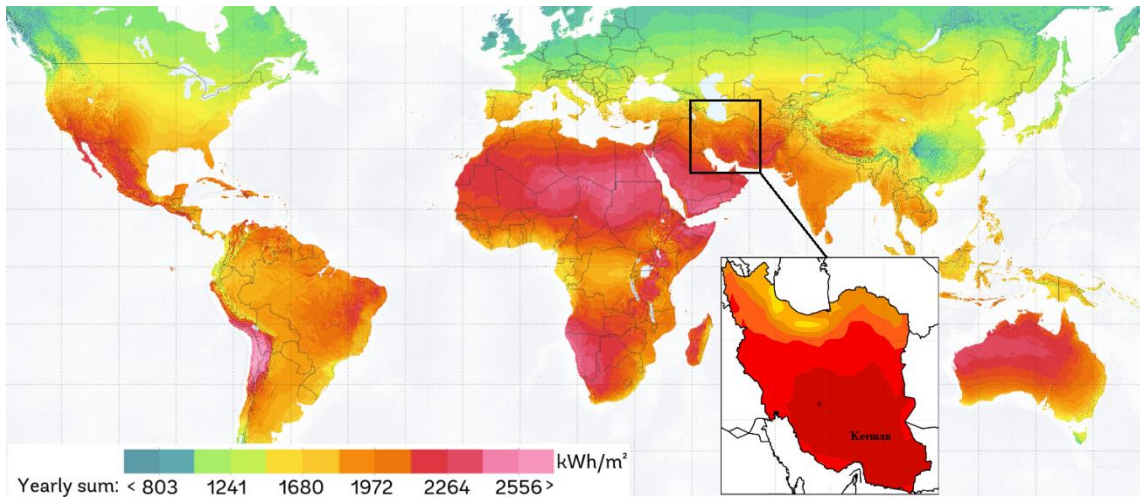
551

552

553

554

555



556

557 Fig. 1: Comparing Annual solar radiance of Kerman with the rest of the world (kWh/m) [39].

558

559

560

561

562

563

564

565

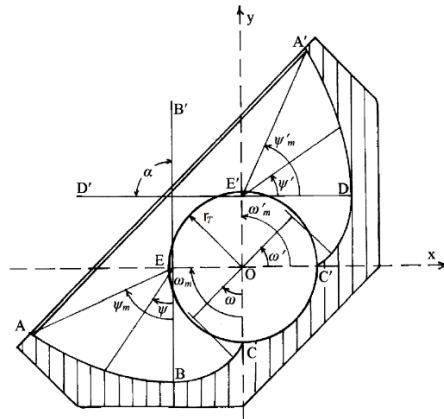
566

567

568

569

570



571

572

573

Fig. 2: Cross-section view of a symmetric CPC [22]

574

575

576

577

578

579

580

581

582

583

584

585



586



587

588

Fig. 3: Construction and assembling the ICS SWH system

589

590

591

592

593

594

595

596

597

598

599



600

601

Fig. 4: The constructed ICS SWH at the testing site in Kerman

602

603

604

605

606

607

608

609

610

611

612

613

614
615
616
617
618
619
620
621
622
623
624
625
626
627
628
629
630
631

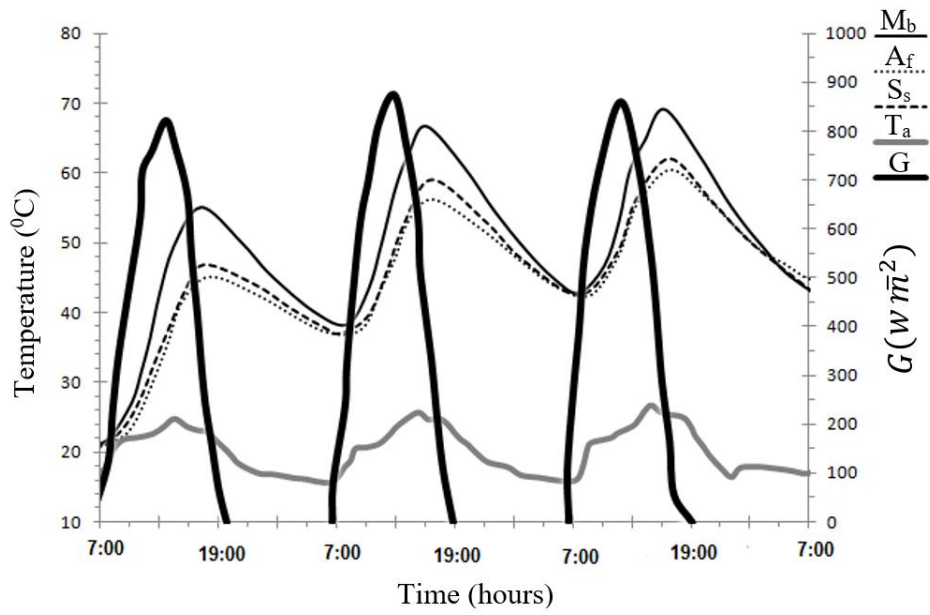
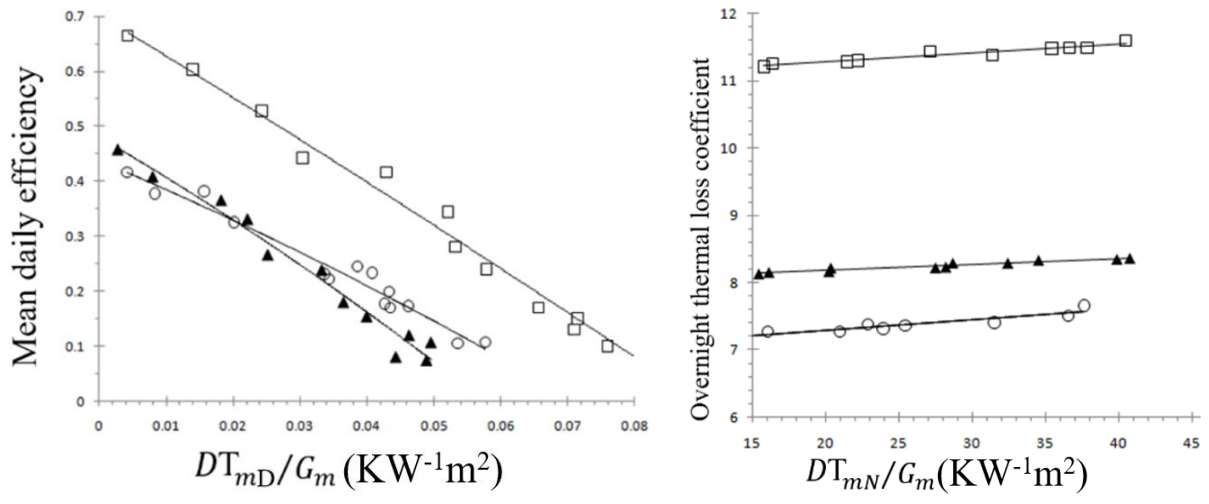


Fig. 5 - Temperature changes for three consecutive days (Mb: Mirror booster , Af: Aluminum foil, Ss: Steel sheet, Ta: ambient temperature , G: incoming solar radiation intensity)

632



633

634

Fig. 6 – Overnight thermal loss coefficients and mean daily efficiency (Mb: □, Ar: ○, Ss: ▲)

635

636

637

638

639

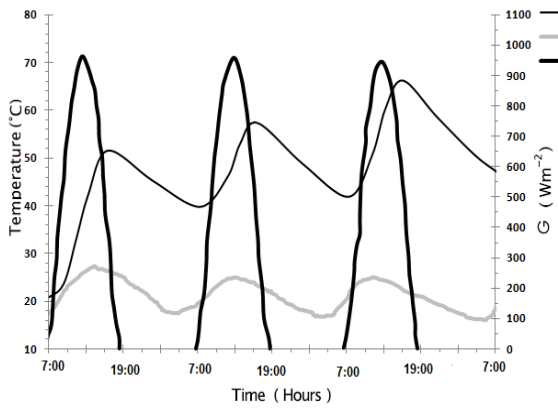
640

641

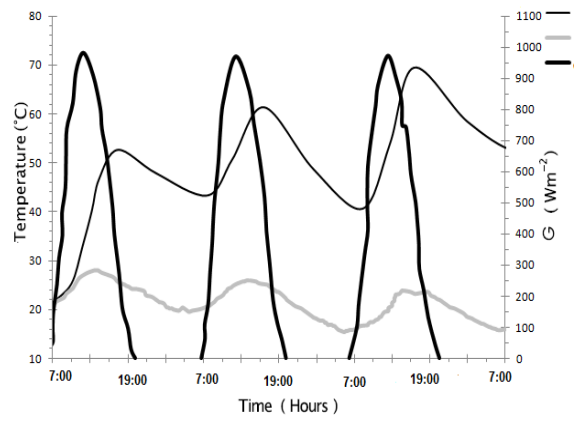
642

643

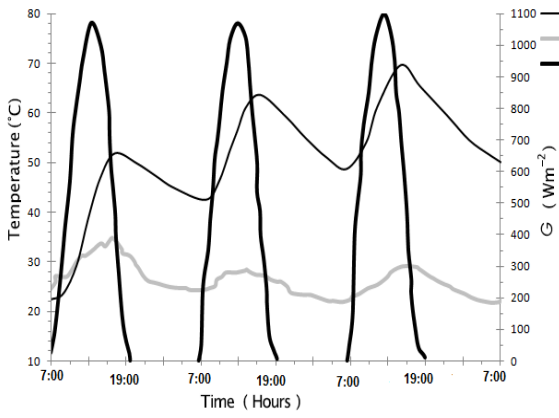
644



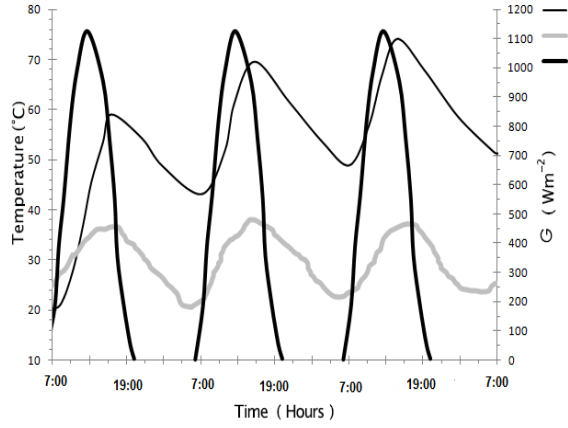
April



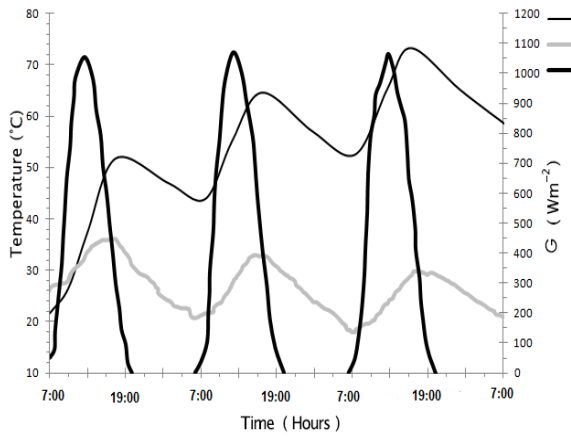
May



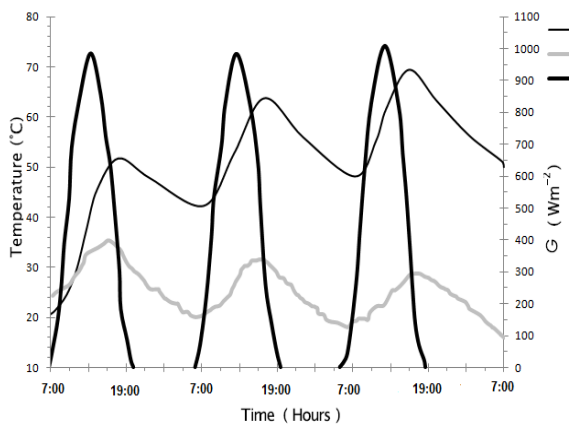
June



July

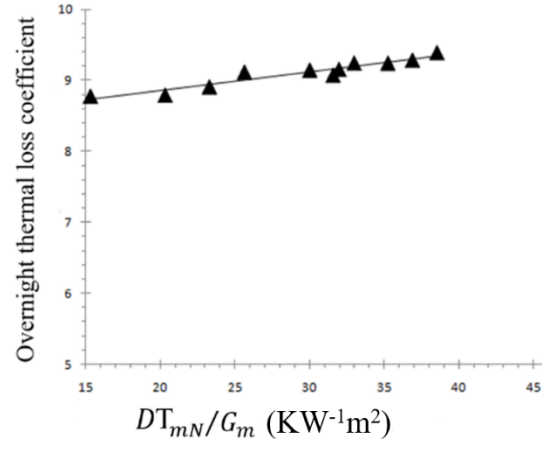
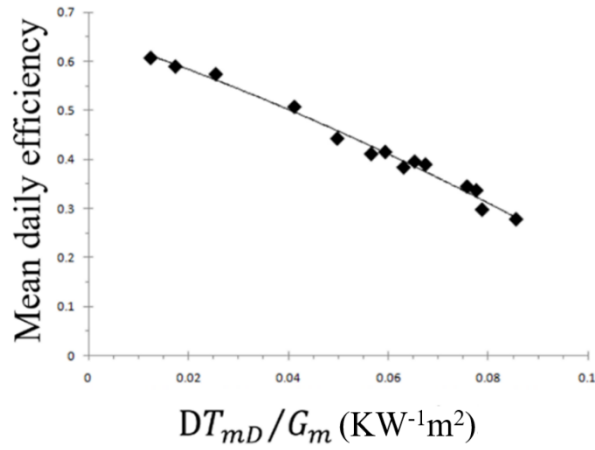


August



September

Fig. 7 – Tw **—**, Ta **—** and G **—** for three consecutive days in 6 different months



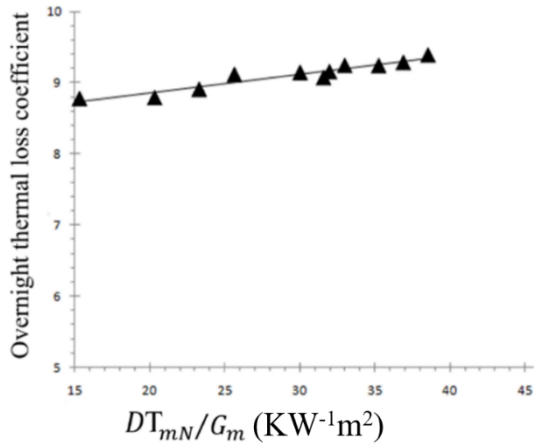
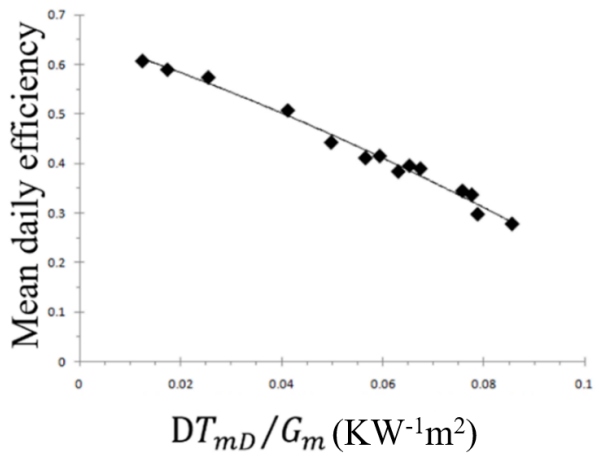
646

647

648

April

649



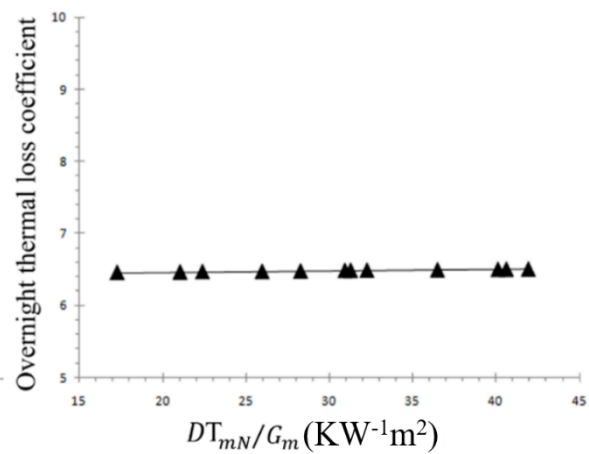
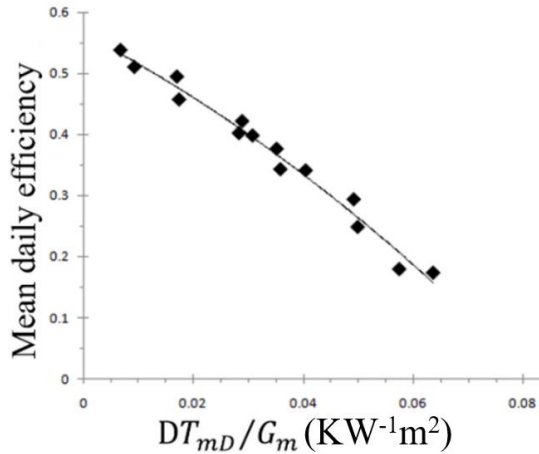
650

651

May

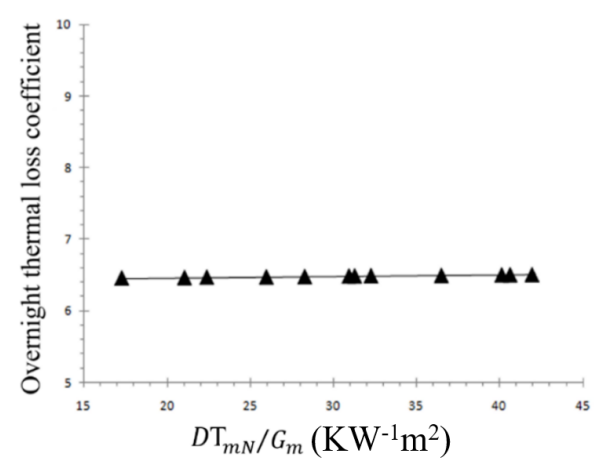
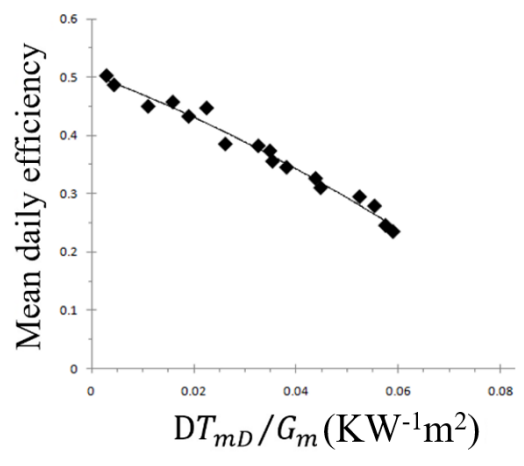
652

653



654
655
656
657

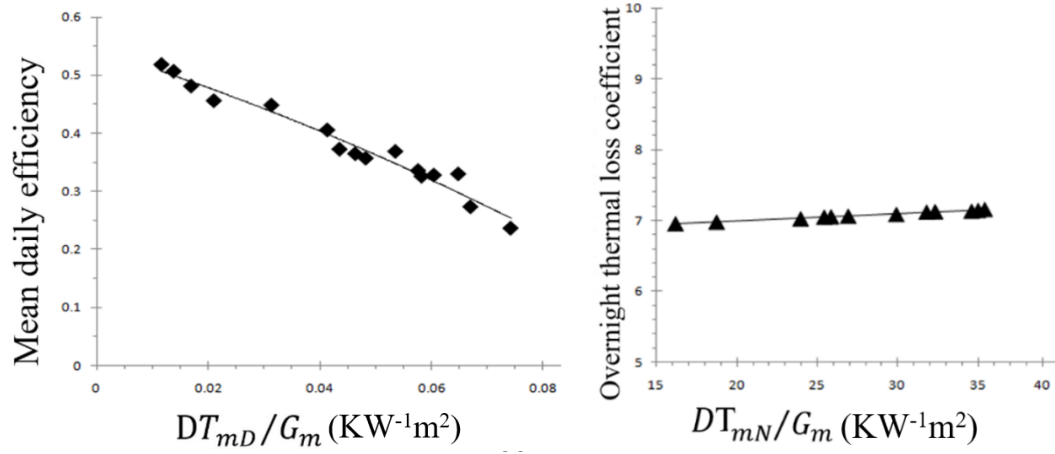
June



663
664
665

July

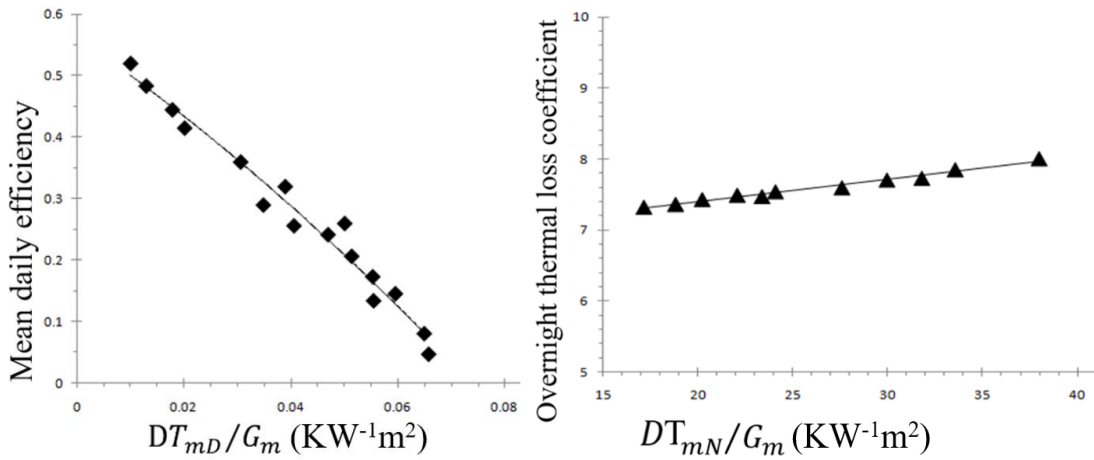
666



668

August

669



670

671

672

673

September

674 Fig. 8 – Mean daily efficiency (left) and heat loss coefficient (right) of ICS SHW in Kerman (6

675 mounts)

676
677
678
679
680
681
682
683
684
685
686
687
688
689
690
691
692
693
694

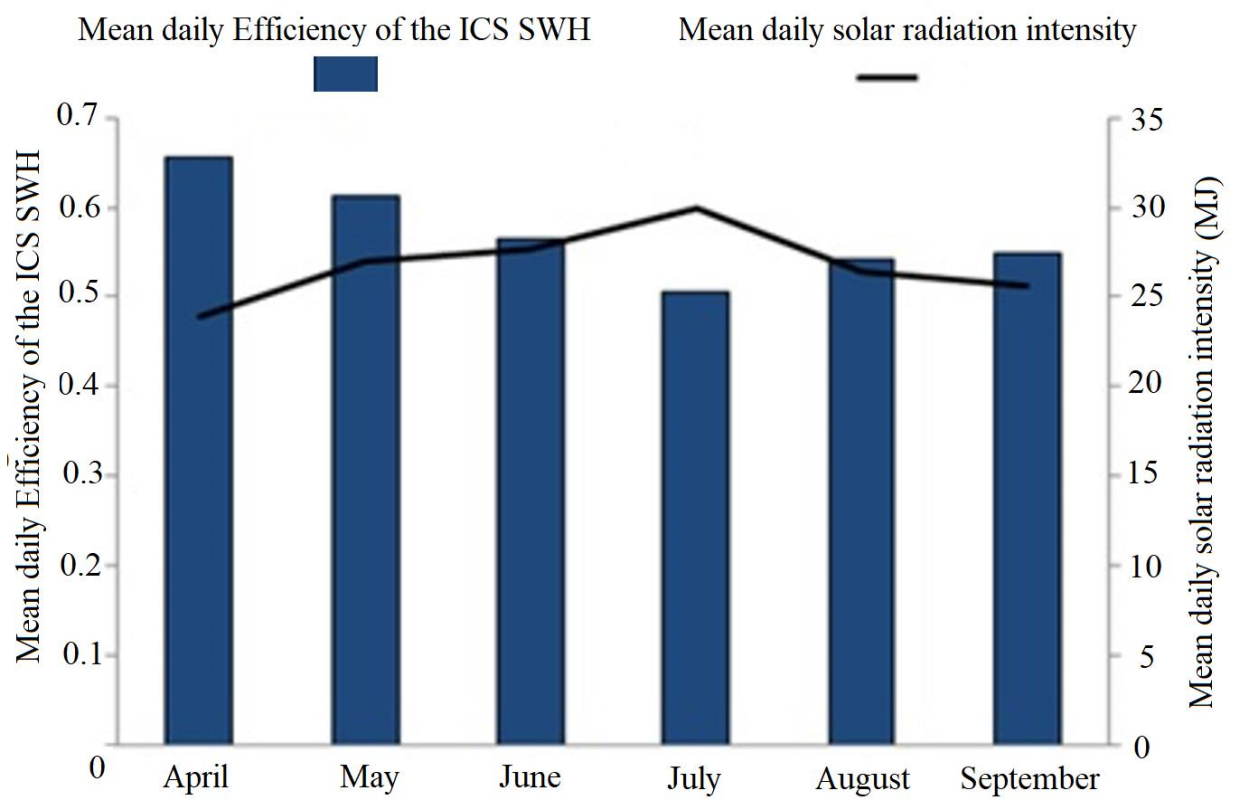


Fig. 9 – Thermal efficiency of the ICS SWH and mean daily radiation in 6 different months in Kerman, Iran

695

696

697

698

Table 1: Configuration details of the tested ICS SWH

D_T	V_T	W_α	A_α	A_r	$\frac{V_T}{A_\alpha}$	CR
30 cm	140 liter	82 cm	16500 cm ²	14100 cm ²	84/64	1/17

699

700

701

702

703

704

705

706

707

708

709

710

711

Table 2 : General characteristics of the water heater

Complete system	Dimension	200×64×113 cm
	Aperture area of systems	1.89 m ²
	Material of aperture	Simple flute glass
Concentrator	Kind of concentrator	CPC
	Material of concentrator	Steel sheet, aluminum foil, and mirror booster
Storage tank	Capacity	140 liters
	Material	Galvanized sheet
	Insulating material	Black enamel

712

713

714

715

716

717

718

719

720

721

722

Table 3. Equations of mean daily efficiency of concentrators

Material	Mean daily efficiency equation η_d	Coefficient of determination
Mirror booster	$\eta_d = 0.667 - 7.4215(DT_{mD}/G_m) - 4.418(DT_{mD}/G_m)^2$	$R^2 = 0.9443$
Steel sheet	$\eta_d = 0.5262 - 8.2903(DT_{mD}/G_m) - 11.561(DT_{mD}/G_m)^2$	$R^2 = 0.9490$
Aluminum foil	$\eta_d = 0.4872 - 5.128(DT_{mD}/G_m) - 14.072(DT_{mD}/G_m)^2$	$R^2 = 0.9574$

723

724

725

726

727

728

729

730

731

732

733

734

735

Table 4: Equations of overnight thermal loss coefficient (U_s) for different concentrators

Material	Mean daily efficiency equation η_d	Coefficient of determination
Mirror booster	$U_s = 11.016 + 0.0132(DT_{mN}/G_m)$	$R^2 = 0.8081$
Steel sheet	$U_s = 8.0035 + 0.009(DT_{mN}/G_m)$	$R^2 = 0.8742$
Aluminum foil	$U_s = 6.9877 + 0.0153(DT_{mN}/G_m)$	$R^2 = 0.7789$

736

737

738

739

740

741

742

743

744

745

Table 5 - The solar slope angles in degree (°) at different months for 6 cities in Iran [50]						
Month	Zahedan	Birjand	Shiraz	Tabas	Yazd	Kerman
January	54.14	58.37	54.64	57.69	56.72	52.83
February	44.00	47.60	40.48	47.82	47.59	2.31
March	30.01	33.28	26.22	33.07	32.50	27.83
April	14.71	17.25	13.34	17.87	16.65	14.55
May	0.97	3.89	1.31	4.68	2.98	1.77
June	-5.28	-2.80	-5.23	-1.94	-3.91	-4.89
July	-2.74	-0.10	-2.07	0.88	-0.97	-2.08
August	9.02	12.24	8.79	12.65	11.32	9.83
September	25.53	28.92	24.96	28.80	28.21	26.63
October	40.64	43.66	39.57	44.32	44.04	41.76
November	52.75	55.92	51.01	55.97	54.72	54.67
December	56.62	60.94	57.50	60.15	58.80	58.62

746

747

748

749

750

751

752

753

754

755

756

757

Table 6: The system's mean daily efficiency (η_d) in different months in Kerman

Months	Mean daily efficiency equation η_d	Coefficient of determination
April	$\eta_d = 0.6557 - 3.3923(DT_{mD}/G_m) - 11.483(Dt_{mD}/G_m)^2$	$R^2 = 0.9760$
May	$\eta_d = 0.6129 - 4.4034(DT_{mD}/G_m) - 6.1728(DT_{mD}/G_m)^2$	$R^2 = 0.9712$
June	$\eta_d = 0.5647 - 4.6561(DT_{mD}/G_m) - 27.468(DT_{mD}/G_m)^2$	$R^2 = 0.9585$
July	$\eta_d = 0.5046 - 3.3051(DT_{mD}/G_m) - 18.606(DT_{mD}/G_m)^2$	$R^2 = 0.9643$
August	$\eta_d = 0.5429 - 2.9902(DT_{mD}/G_m) - 12.211(DT_{mD}/G_m)^2$	$R^2 = 0.9206$
September	$\eta_d = 0.5525 - 5.9753(DT_{mD}/G_m) - 22.128(DT_{mD}/G_m)^2$	$R^2 = 0.9663$

758

759

760

761

762

763

Table 7: Overnight heat loss coefficient of the system (U_s) in different months in Kerman

Months	Mean daily efficiency equation η_d	Coefficient of determination
April	$U_s = 8.3357 + 0.0261(DT_{mN}/G_m)$	$R^2 = 0.9648$
May	$U_s = 7.1134 + 0.0223(DT_{mN}/G_m)$	$R^2 = 0.9444$
June	$U_s = 6.4208 + 0.0019(DT_{mN}/G_m)$	$R^2 = 0.8447$
July	$U_s = 5.7184 + 0.0152(DT_{mN}/G_m)$	$R^2 = 0.9259$
August	$U_s = 6.7821 + 0.0102(DT_{mN}/G_m)$	$R^2 = 0.8542$
September	$U_s = 6.79 + 0.0315(DT_{mN}/G_m)$	$R^2 = 0.9677$

764

765

766

767

768

769

770

771

772

773

Abbreviation

D_T	Diameter of storage tank (cm)	A_α	Area of aperture (cm ²)
V_T	Volume of storage tank (liter)	A_r	Area of absorber (cm ²)
CR	Concentration Ratio	C	Maximum mean daily efficiency coefficient
ICS	Integrated collector storage	Q_W	Heat in the tank of water storage (J)
SWH	Solar water heater	Q_R	Integrated solar radiation on the aperture of the system (J)
η_d	Mean daily efficiency	T_{mN}	Mean water temperature difference during the night
r_T	Radius of storage tank	A	Acceptance angle of the system (°, rad)
DT_{mD}	Mean water temperature difference during the day	Dt_D	Time interval during daily operation
CPC	Compound-parabolic-concentrator	T_a	Ambient temperature
W_α	Width of concentrator	G	Incoming solar radiation intensity
L_T	Length of storage tank	D_t	Time interval
L_α	Length of aperture	U_s	Coefficient of thermal losses during the night
M_w	Mass of water	G_m	Mean daily solar radiation intensity
$C_{p,w}$	Specific heat of water	T_0	Initial storage water temperature
A_f	Aluminum foil	t_0	Initial time
T_1	Final storage water temperature	t_1	Final time
T_{ma}	Average ambient temperature	S_s	Steel sheet
M_b	Mirror booster	DT_{mN}	Mean water temperature difference during the night
ω	Involute concentrator's angle (°, rad)	Ψ	Parabolic concentrator's angle (°, rad)
$\acute{\omega}$	Upper involute concentrator's angle (°, rad)	$\acute{\Psi}$	Upper parabolic concentrator's angle (°, rad)